University of Groningen

A porcine model of heart failure with preserved ejection fraction

Charles, Christopher J.; Lee, Philip; Li, Renee R.; Yeung, Teresa; Mazlan, Stephane M. Ibraham; Tay, Zhi Wei; Abdurrachim, Desiree; Teo, Xing Qi; Wang, Wei-Hsin; de Kleijn, Dominique P.

IMPORTANT NOTE: You are advised to consult the publisher's version (publisher's PDF) if you wish to cite from it. Please check the document version below.

Document Version
Publisher's PDF, also known as Version of record

Publication date:
2019

Link to publication in University of Groningen/UMCG research database

ORIGINAL RESEARCH ARTICLE

A porcine model of heart failure with preserved ejection fraction: magnetic resonance imaging and metabolic energetics

Christopher J. Charles[1,2,3]*, Philip Lee[4], Renee R. Li[1,2], Teresa Yeung[1,2], Stephane M. Ibraham Mazlan[1,2], Zhi Wei Tay[4], Desiree Abdurrachim[4], Xing Qi Teo[4], Wei-Hsin Wang[4], Dominique P.V. de Kleijn[5,6], Patrick J. Cozzone[4], Carolyn S.P. Lam[1,7,8,9,10] and A. Mark Richards[1,3]

[1]Cardiovascular Research Institute, National University Heart Centre, Singapore; [2]Department of Surgery, Yong Loo Lin School of Medicine, National University of Singapore, Singapore; [3]Christchurch Heart Institute, University of Otago, Christchurch, New Zealand; [4]Singapore Bioimaging Consortium, Agency for Science, Technology and Research, Singapore; [5]Department of Vascular Surgery, University Medical Centre, Utrecht, Utrecht, The Netherlands; [6]Netherlands Heart Institute, Utrecht, The Netherlands; [7]National Heart Centre Singapore, Singapore; [8]Faculty of Medicine, Duke-National University Singapore, Singapore; [9]University Medical Centre Groningen, Gronigen, The Netherlands; [10]The George Institute for Global Health, Sydney, Australia

Abstract

Aims   A significant proportion of heart failure (HF) patients have HF preserved ejection fraction (HFpEF). The lack of effective treatments for HFpEF remains a critical unmet need. A key obstacle to therapeutic innovation in HFpEF is the paucity of pre-clinical models. Although several large animal models have been reported, few demonstrate progression to decompensated HF. We have established a model of HFpEF by enhancing a porcine model of progressive left ventricular (LV) pressure overload and characterized HF in this model including advanced cardiometabolic imaging using cardiac magnetic resonance imaging and hyperpolarized carbon-13 magnetic resonance spectroscopy.

Methods and results   Pigs underwent progressive LV pressure overload by means of an inflatable aortic cuff. Pigs developed LV hypertrophy (50% increase in wall thickness, $P < 0.001$, and two-fold increase in mass compared to sham control, $P < 0.001$) with no evidence of LV dilatation but a significant increase in left atrial volume ($P = 0.013$). Cardiac magnetic resonance imaging demonstrated T1 modified Look-Locker inversion recovery values increased in 16/17 segments compared to sham pigs ($P < 0.05$–$P < 0.001$) indicating global ventricular fibrosis. Mean LV end-diastolic ($P = 0.047$) and pulmonary capillary wedge pressures ($P = 0.008$) were elevated compared with sham control. One-third of the pigs demonstrated clinical signs of frank decompensated HF, and mean plasma BNP concentrations were raised compared with sham control ($P = 0.008$). Cardiometabolic imaging with hyperpolarized carbon-13 magnetic resonance spectroscopy agreed with known metabolic changes in the failing heart with a switch from fatty acid towards glucose substrate utilization.

Conclusions   Progressive aortic constriction in growing pigs induces significant LV hypertrophy with cardiac fibrosis associated with left atrial dilation, raised filling pressures, and an ability to transition to overt HF with raised BNP without reduction in LVEF. This model replicates many aspects of clinical HFpEF with a predominant background of hypertension and can be used to advance understanding of underlying pathology and for necessary pre-clinical testing of novel candidate therapies.

Introduction

Heart failure (HF) is the final common pathway of a myriad of metabolic and cardiovascular diseases and imposes a significant healthcare burden worldwide. Although there have been

significant improvements in clinical management and outcomes, morbidity and mortality remain high, and there is an indisputable need for improved treatment options. The pathophysiology of HF is complex. Whilst many patients present clinically as HF with reduced ejection fraction (HFrEF) (≤40%

EF), a significant proportion of HF patients have preserved EF (HFpEF) demonstrating a reduced ability of the heart to relax but with EF above 50%.")[OAurl][?–]>")[OAurl][?–]>[1] Our recently reported prospective multi-ethnic study shows that HFpEF accounts for ~30% of all HF cases in parallel New Zealand and Singapore cohorts. HFpEF is characterized by older age, a greater prevalence of females, and predominant background hypertension (78%) compared with HFrEF.")[OAurl][?–]>")[OAurl][?–]>[2] Two year mortality was lower than HFrEF but still high at 14% and the composite outcome of all-cause mortality or HF hospitalization occurring in 35%.

Clinical trials in patients with HFpEF have failed to demonstrate improvements in mortality. A recent meta-analysis examining data from 25 trials (>18 000 patients) showed no beneficial effect from angiotensin-converting enzyme inhibitors, angiotensin receptor blocker, or mineralocorticoid antagonists on mortality or HF hospitalization.")[OAurl][?–]>")[OAurl][?–]>[3] The lack of effective treatments for HFpEF remains a critical unmet need. A significant obstacle to therapeutic innovation in HFpEF is the absence of pre-clinical models including large animal models that, unlike rodent models, permit detailed instrumentation and extensive imaging and sampling protocols.")[OAurl][?–]>")[OAurl][?–]>[4] Although several large animal models have been reported,")[OAurl][?–]>")[OAurl][?–]>[5] none fulfil all the features present in human disease, and few demonstrate progression to HF. We hypothesized that enhancing a porcine model of progressive left ventricular pressure overload (LVPO)")[OAurl][?–]>")[OAurl][?–]>[6] with greater characterization would demonstrate incipient HF with some animal progressing to definitive HF confirming that this model is suitable for ongoing pre-clinical studies of HFpEF. Accordingly, we established and enhanced this model of LVPO and characterized HF in this model with clinical observations, filling pressures and BNP measurements and also advanced cardiometabolic imaging using cardiac magnetic resonance imaging (CMRI) and hyperpolarized carbon-13 magnetic resonance (HP[13]CMR) spectroscopy.

Materials and methods

The study protocol was approved by the Institutional Animal Care and Use Committees of National University of Singapore and Biological Research Centre, Agency for Science, Technology and Research. We built on a previously reported progressive LVPO model")[OAurl][?–]>")[OAurl][?–]>[6] with key enhancements to progress pigs to evidence-based HFpEF. Thirty-nine female Yorkshire × Landrace pigs (18–23 kg) were housed individually receiving standard care.

For echocardiography and CMRI, pigs were pre-medicated with intramuscular ketamine (Ceva Animal Health, Glenorie NSW, Australia) (10 mg/kg), atropine (Atrosite, Troy Laboratories, Glendenning NSW, Australia) (0.04 mg/kg), and midazolam (Dormicum, Hoffmann-La Roche, Basel, Switzerland)

(0.6 mg/kg), intubated, ventilated, and maintained with inhalation isoflurane (Attane, Piramal Critical Care, Bethlehem, PA). Following Day 0 imaging, pigs were switched to total intravenous (i.v.) anaesthesia [midazolam 2.5–4 mg/kg/h, alfentanil (Rapifen, GlaxoSmithKline, Torrile, Italy) 250–400 µg/kg/h, and pancuronium (Rotexmedica, Trittau, Germany) 0.25–0.3 mg/kg/h] for surgical implantation of aortic cuff. Other medications included oral amiodarone (Cordarone, Sanofi-Aventis, Paris, France) (200 mg daily), clopidogrel (Ceruvin Ranbaxy, Kedah, Malaysia) (75–300 mg), and aspirin (Cardiprin, Reckitt Benckiser Healthcare, Hull, UK) (100 mg daily). Pigs also received augmentin (SmithKline Beecham, Worthing, UK) (15 mg/kg i.v. then 312 mg orally for 5 days) and fentanyl (Durogesic®, Janssen Pharmaceutica, Beerse, Belgium) transdermal patches (5 µg/h for 4 days). All pigs underwent left lateral thoracotomy and pericardiotomy to isolate the aorta. In 33 pigs, an inflatable cuff (Access Technologies, Skokie, IL, www.norfolkaccess.com) was placed around the aortic root and connected to an injectable port tunnelled subcutaneously adjacent to the scapula. Sham pigs (*n* = 6) had thoracotomy without cuff placement. Pigs recovered for 1 week prior to commencement of cuff inflation.

Pigs underwent weekly echocardiography prior to progressive cuff inflation over 4 weeks titrated to achieve incremental trans-constriction pressure gradients (PGs) of 20, 40, 60, and 80 mmHg (assessed echocardiographically). From week 4, the PG was maintained at 80 mmHg until completion of final magnetic resonance imaging (MRI) and HP[13]CMR measurements after which pigs were terminated. Cardiac left ventricle (LV) and lungs were excised, weighed, and samples taken for subsequent histology. Sham pigs underwent identical procedures. Trans-thoracic and trans-oesophageal echo were used to acquire standard cardiac structure and function measures (Philips EPIQ7 machine). Trans-oesophageal echo, with tissue Doppler imaging, of the aortic root displayed the cuff-induced aortic constriction and defined PGs enabling titration of cuff inflation up or down as necessary.

CMRI was performed prior to thoracotomy and repeated either Day 35 or Day 42 (sham and 2nd half cuff pigs) using Siemens 3T MRI scanner (MAGNETOM Skyra, Siemens Healthineers AG, Erlangen, Germany). Standard CMRI protocol included cine imaging [global and regional LV systolic function including LV volumes, mass, and LV ejection fraction (LVEF)], and T1-mapping from Modified Look-Locker Imaging (MOLLI). MRI analysis was performed using SEGMENT v2.2 R6338 (http://segment.heiberg.se). A subset of pigs underwent tandem CMRI and CMRI hyperpolarizer on Day 42.

HP[13]CMR spectroscopy was performed in the same scanner as CMRI, using 13C TX quadrature volume coil/13C RX 16-channel flex array coil (Rapid Biomedical, Rimpar, Germany). [1-13C]pyruvate (7.18 mmol/L; Cambridge Isotope Laboratories) doped with AH111501 (15 mM) was inserted into polarizer (SPINLab, GE Healthcare, Chicago, IL) for microwave irradiation. The polarized sample was subsequently

dissoluted yielding a solution of 250 mmol/L [1-13C]pyruvate (pH = 7.2–7.7) for immediate injection into animals at a dose of 0.2 mmol/kg body weight. ^{13}C-MRS started just before i.v. bolus injection of hyperpolarized [1-13C]pyruvate. The build-up of metabolites was followed for ~2 min after injection, with spectra sampled every two heartbeats. Quantification of metabolites was performed using AMARES in the jMRUI software package (http://www.jmrui.eu).")[OAurl][?–]>")[OAurl][?–]>[7],^{13}C-MR spectra were summed over 40 s upon metabolite appearance with peaks fitted for [1-13C]lactate, [1-13C]pyruvate hydrate, [1-13C]alanine, and [13C]bicarbonate all normalized to the [1-13C]pyruvate peak.

Ethylenediaminetetraacetic acid blood samples drawn at baseline and pre-termination were centrifuged, and plasma was stored at -80^0C prior to assay for porcine BNP at Christchurch Heart Institute using a well-validated assay.")[OAurl][?–]>")[OAurl][?–]>[8] A subset of pigs (six sham and five cuff) underwent invasive pressure monitoring immediately after final echocardiography. Sheaths were placed in a jugular vein and carotid artery to allow passing under fluoroscopic guidance a Swan Ganz catheter into the pulmonary artery for measurement of pulmonary capillary wedge pressure (PCWP) and a fluid-filled catheter into the LV for measurement of end-diastolic pressure (LVEDP). LV tissue harvested post-mortem was fixed in buffered 10% formaldehyde prior to paraffin embedding. Picrosirius red staining was performed

by standard methods to allow assessment of myocardial fibrosis using automated image analysis (IMAGEJ).

Statistics

Results are expressed as mean ± standard error of mean. Primary analysis was independent *t*-tests of time-matched data between the sham and cuff pigs. $P < 0.05$ was the threshold for statistical significance.

Results

Studies in sham pigs proceeded as planned with data collection complete. Among the cuff-implanted pigs, three experienced cuff failure (Days 21–28) and were excluded from analyses. A further five pigs were excluded due to premature death (<Day 28) with post-mortems revealing two fatal aortic occlusion deaths (last recorded PG >80 mmHg), one aortic rupture, one with large aortic and LV thrombi, and one pig died of bacterial pneumonia. A further five pigs successfully completed the protocol but exhibited no significant increase in LV mass despite equivalent PGs. Since LV hypertrophy (LVH) was the primary driver for development of HFpEF, these pigs were also excluded from further analysis. Twenty

Figure 1 Serial body weight, pressure gradients across aortic arch, left ventricular mass/body weight (LV$_{mass}$/BW) ratios, and echocardiography derived serial left ventricular dimensions including interventricular septum thickness at diastole, left ventricular posterior wall thickness at diastole and left ventricular internal diameter at diastole in 20 pigs with progressive inflation of aortic cuff to induce left ventricular hypertrophy (●) and six sham control (○) pigs. Values shown are mean ± standard error of the mean. Significant differences at time-matched points between the sham and aortic cuff to induce left ventricular hypertrophy pigs are indicated as follows: *$P < 0.05$, **$P < 0.01$ and ***$P < 0.001$.
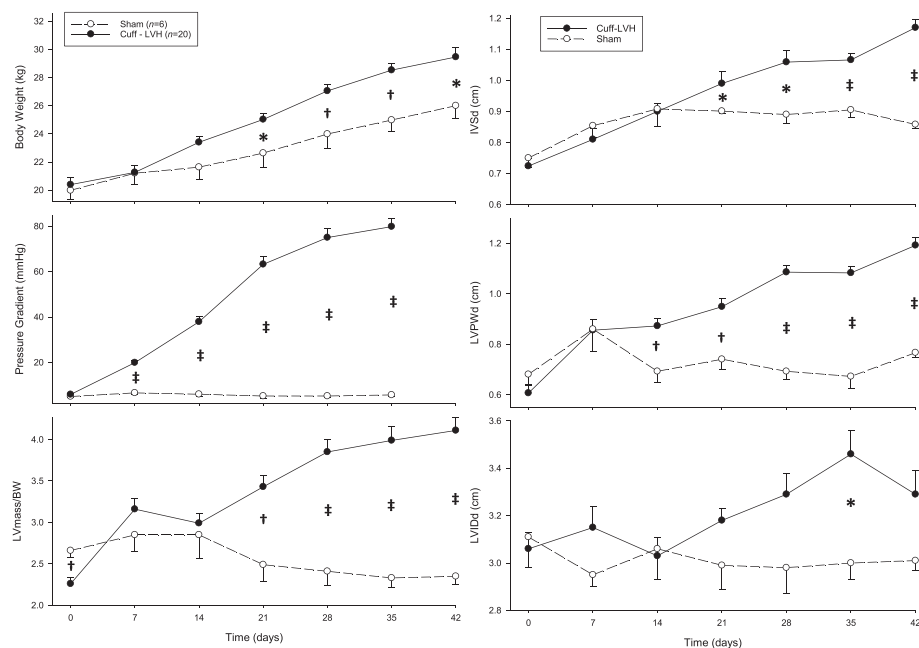
pigs undergoing aortic cuffing completed the full protocol and developed LVH (cuff-LVH group). Data from this group are compared to animals undergoing sham procedures.

Both sham and cuff-LVH pigs gained weight throughout the protocol (*Figure* ")[OAurl][?–]>")[OAurl][?–]>*1*). The PG remained minimal (<6 mmHg) in the sham group but rose stepwise (in ~20 mmHg increments) over 4 weeks and thereafter remained stable (*Figure* ")[OAurl][?–]>")[OAurl][?–]>*1*).

From 2 weeks, LV mass indexed to body weight (LV_{mass}/BW) increased in the cuff-LVH group to be significantly (~two-fold) higher than sham controls by the end of the study (*Figure* ")[OAurl][?–]>")[OAurl][?–]>*1*). Measures of LV mass by echocardiography, CMRI, and direct weighing at post-mortem correlated well. LV wall dimensions were stable in sham pigs but increased in the cuff-LVH pigs. Thickness of both interventricular septums and LV posterior walls in diastole increased in the cuffed pigs to be significantly higher than sham by Day 21 and eventually ~50% thicker (*Figure* ")[OAurl][?–]>")[OAurl][?–]>*1*). The LV internal diameter
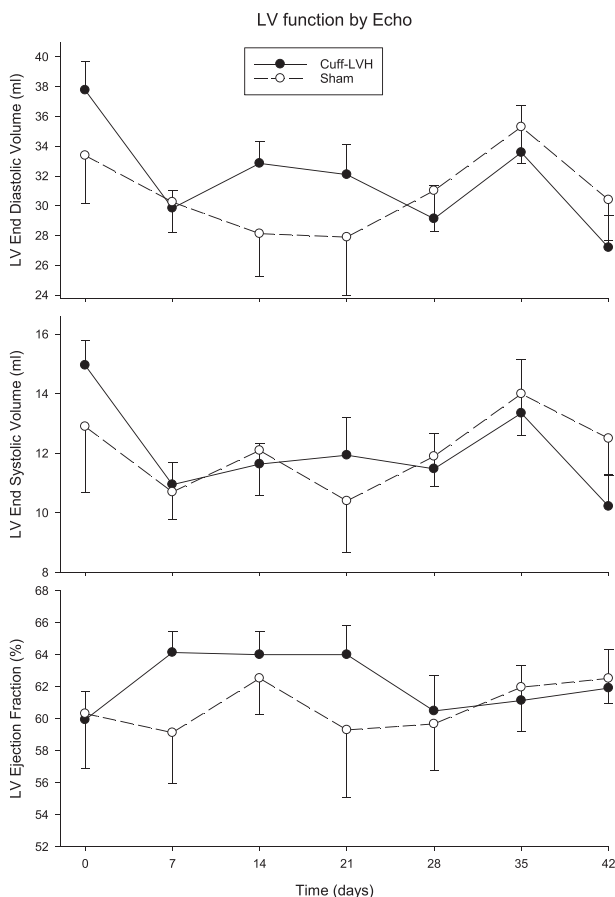
showed some increase in the cuff group, but the dimension was only greater than sham at Day 35 (*Figure* ")[OAurl][?–]>")[OAurl][?–]>*1*).

LVEF remained stable with values for both sham and LVH-cuff group remaining in the 60–65% range (*Figure* ")[OAurl][?–]>")[OAurl][?–]>*2*). There was no significant change in either group in LV end-systolic volumes (LVESVs) or LV end-diastolic volumes (LVEDVs) (*Figure* ")[OAurl][?–]>")[OAurl][?–]>*2*). LV structure and function data measured by CMRI at baseline and the end of study corroborated changes measured by echocardiography with no significant changes comparing cuff-LVH to sham pigs for LVEDV, LVESV, stroke volume, LVEF, cardiac output, or peak ejection rate (*Figure* ")[OAurl][?–]>")[OAurl][?–]>*3*). In contrast, left atrial end-diastolic volume (*P* = 0.013 compared to baseline) and peak filling rate (*P* < 0.01 compared with sham) increased in the cuff-LVH (*Figure* ")[OAurl][?–]>")[OAurl][?–]>*3*).

Native T1 values derived from MOLLI did not differ significantly between sham and cuff-LVH pigs at Day 0 for 16/17 segments of the LV (with the mid-inferior segment the exception; *Figure* ")[OAurl][?–]>")[OAurl][?–]>*4A*). By the end of study T1 values were significantly higher in the cuff-LVH pigs compared with sham for 16/17 segments with the apical-lateral segment the sole exception. Picrosirius red staining of sections from LV free wall (*Figure* ")[OAurl][?–]>")[OAurl][?–]>*4B*) showed an increase in both interstitial and perivascular collagen deposition in the tissue from the cuff-LVH pig with mean intensities measured under a bright field showing a trend for difference and under polarized light being significantly different (*P* = 0.044) between LVH and sham groups.

Invasive intra-cardiac pressures (sub-study) showed normal range pressures in sham pigs, but both PCWP (*P* = 0.008) and LVEDP (*P*= 0.047) were raised in cuff-LVH pigs (*Figure* ")[OAurl][?–]>")[OAurl][?–]>*5*). Plasma BNP levels remained in the normal range in sham control pigs but on average increased by end of study in the cuff-LVH pigs being significantly higher than sham (*P* = 0.008) and baseline (Day 0) values (*P* = 0.02) (*Figure* ")[OAurl][?–]>")[OAurl][?–]>*5*). Clinical signs of HF were observed in at least one-third of the pigs including tachypnea, laboured breathing, cough, lung congestion on auscultation, cyanosis, and lethargy. One pig demonstrated major falls in arterial oxygen saturation (SPO_2 < 40%) on induction of anaesthesia for Day 35 imaging with extreme cyanosis and severe pulmonary oedema and pleural effusions. This pig underwent drainage of accumulated pleural fluid and received additional oxygen therapy and treatment with 2 mg/kg i.v. frusemide (Furosemide Fresenius Kabi, Bad Homburg, Germany) before stabilizing and proceeding to MRI and echo, followed by partial removal of glycerol from the aortic cuff to stabilize PG. It recovered to survive to end of the protocol (Day 42).

Representative cardiac ^{13}C-MR spectra after injection of hyperpolarized [1-13C]pyruvate from a normal (sham) pig

Figure 2 Echocardiography derived serial left ventricular volumes and ejection fraction in 20 aortic cuff to induce left ventricular hypertrophy (●) and six sham control (○) pigs. Values shown are mean ± standard error of the mean.

Figure 3 Cardiac magnetic resonance imaging derived left ventricular end diastolic volume, end systolic volume, stroke volume, ejection fraction, peak filling and ejection rates, cardiac output and left atrial end-diastolic (ED) volume in 20 aortic cuff to induce left ventricular hypertrophy (●) and six sham control (○) pigs. Values shown are mean + standard error of the mean. Left atrial end-diastolic volume was significantly increased at 42 days compared with baseline (*P < 0.05) and left ventricular peak filling rate increased in aortic cuff to induce left ventricular hypertrophy pigs compared with sham (**P < 0.01).
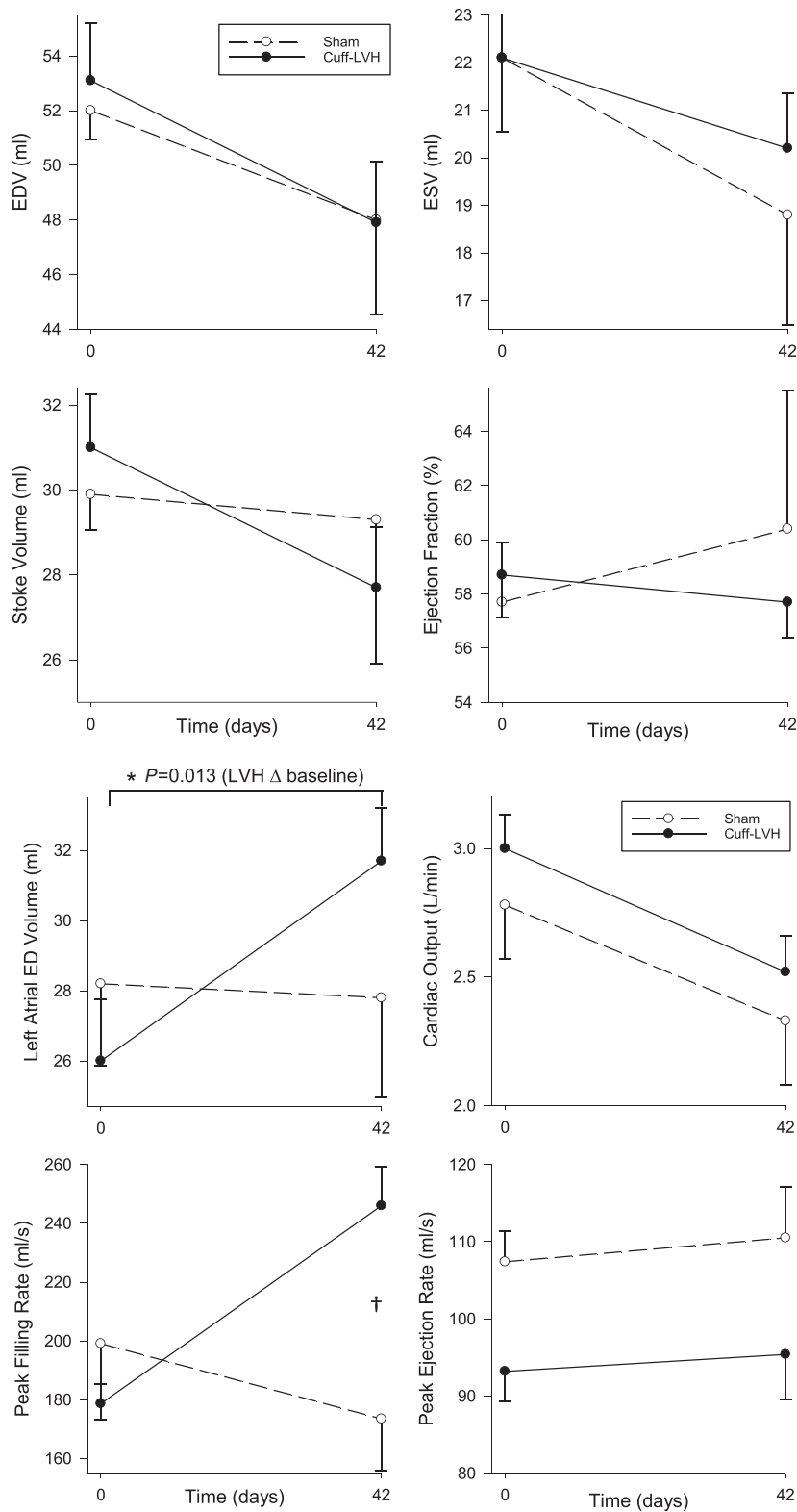
Figure 4 Top panel – cardiac MRI T1 MOLLI values across 17 segments of the LV at baseline and end of study in 20 cuff-LVH (●) and 6 sham control (○) pigs. Bottom panels – examples on picrosirius red staining of sections of the LV free wall and group mean intensities from sham and cuff-LVH pigs measured under bright field and polarizing light. Values shown are mean + SEM. Significant differences at time-matched points between the sham and cuff-LVH pigs are indicated as follows: *$P < 0.05$, †$P < 0.01$ and ‡$P < 0.001$.

Picrosirius Red Staining of LV free wall
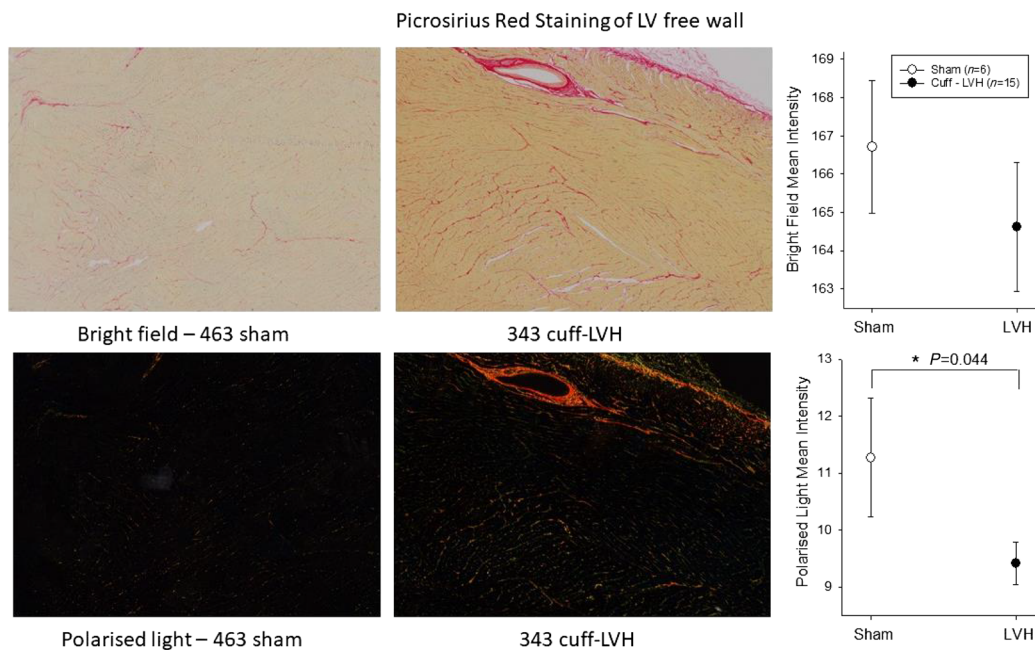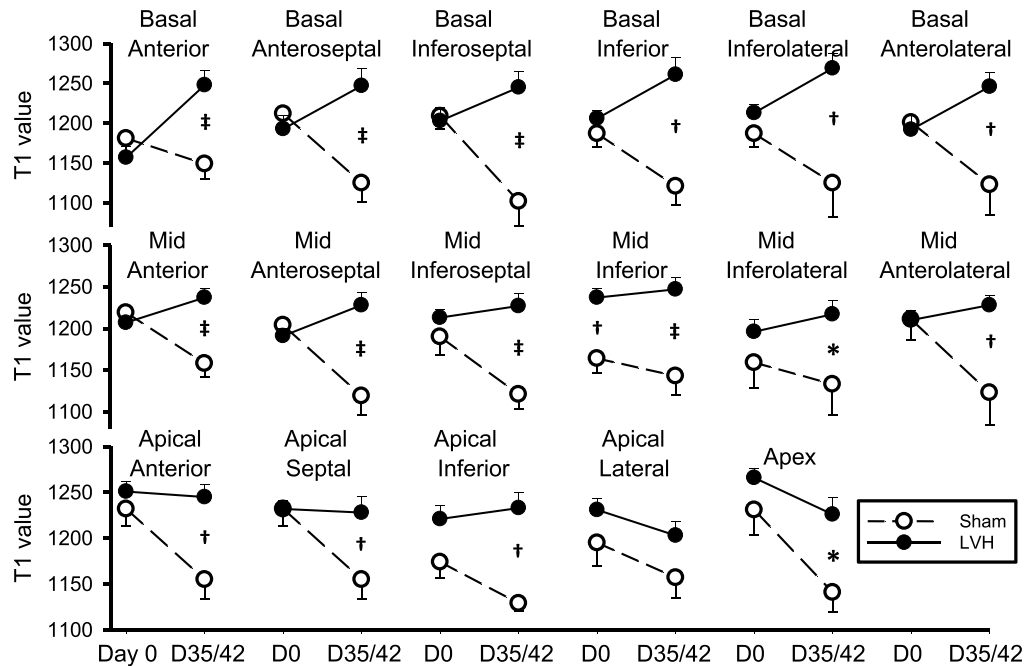
demonstrates that [1-13C]pyruvate is metabolized into [1-13C]lactate, [1-13C]alanine, [13C]bicarbonate via lactate dehydrogenase, alanine aminotransferase (ALT), and pyruvate dehydrogenase (PDH), respectively with metabolic products visible within 2 min (*Figure* "[OAurl][?–]>")[OAurl][?–]>*6A*).

Compared to sham pigs, cuff-LVH pigs showed increases in [1-13C]alanine ($P < 0.01$) and [13C]bicarbonate ($P < 0.05$) with no increase in [1-13C] lactate representing ~2.6-fold and ~6-fold increase in ALT and PDH activity, respectively (*Figure* "[OAurl][?–]>")[OAurl][?–]>*6B*).

Figure 5 Top panels – invasive pulmonary capillary (PC) wedge pressure and LV end diastolic pressure in 5 cuff-LVH (●) and 6 sham control (○) pigs. Lower panels – plasma B-type natriuretic peptide (BNP) levels in cuff-LVH (●) and sham control (○) pigs. Values shown are mean + SEM. Significant differences at time-matched points between the sham and cuff-LVH pigs are indicated as follows: $*P < 0.05$ and $\dagger P < 0.01$.
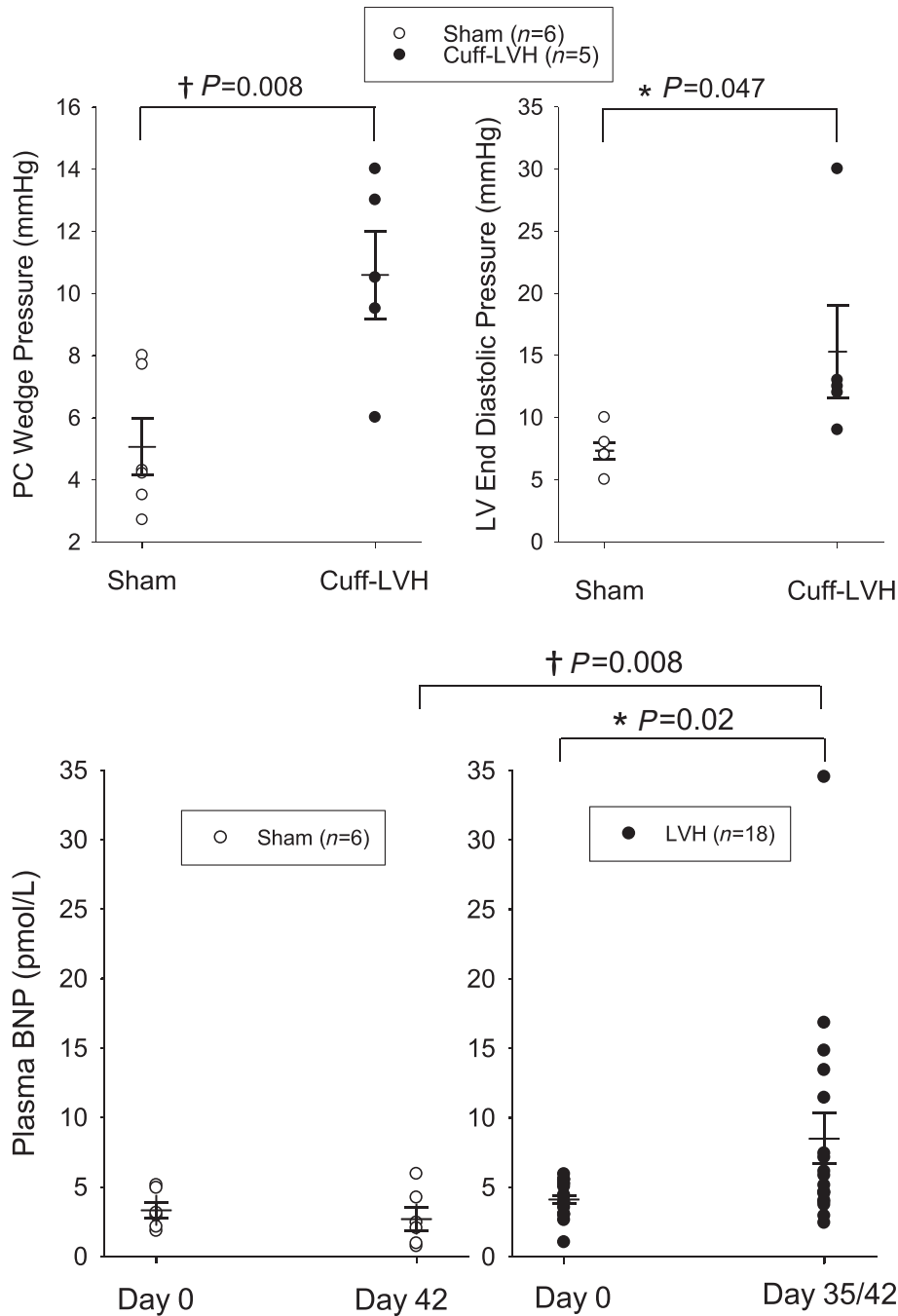
Discussion

This porcine HFpEF model demonstrates significant LVH (doubling of LV mass) without LV dilation similar to that previously reported.")[OAurl][?–]>")[OAurl][?–]>[6] Unique features of our model that document HF include comprehensive serial imaging (echocardiography and MRI) clearly demonstrating global ventricular fibrosis by MRI T1 MOLLI, a significant increases in plasma BNP, and significantly elevated PCWP and LVEDP. Hyperpolarized ^{13}C-MR studies showed increased

Figure 6 Metabolic signals from hyperpolarizing ^{13}C magnetic resonance imaging (A) ^{13}C spectra from a normal (sham) pig and (B) metabolite/pyruvate signal from 11 aortic cuff to induce left ventricular hypertrophy (●) and six sham control (○) pigs. Values shown are mean ± standard error of the mean. The units are in arbitrary units and normalized to the [1-13C] pyruvate peak amplitude of each animal. Significant differences at time-matched points between the sham and aortic cuff to induce left ventricular hypertrophy pigs are indicated as follows: *$P < 0.05$ and **$P < 0.01$.
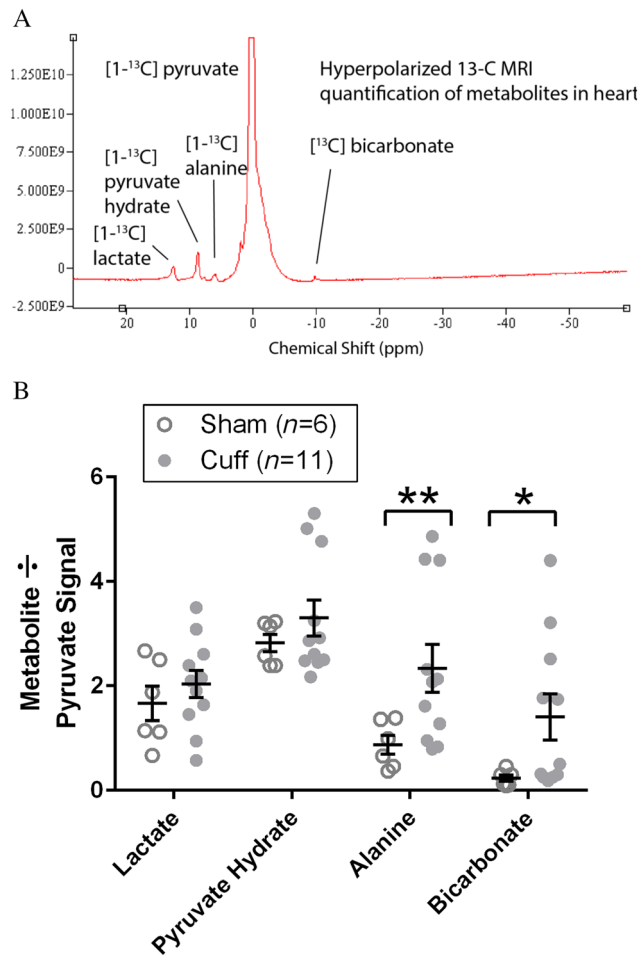
ALT and PDH activity in HFpEF pigs. Pigs developed incipient HF with frequent progression to frank decompensated HFpEF manifested in clinical symptoms, raised LV filling pressures and, in some pigs, frank pulmonary oedema. Taken together, full characterization of this enhanced LVPO model demonstrates development of incipient HF with some animals progressing to overt HF confirming that this provides a clinically relevant model suitable for ongoing preclinical studies of HFpEF.

Our model is based the porcine LVPO model first reported by Spinale et al.")[OAurl][?–]>")[OAurl][?–]>[6] Early development was attended by complications that subsequently became infrequent. Most early deaths were incurred in the early phase of setting up the model. Titration of the cuff

filling was guided by a combination of factors including degree of LVH, measured PG and PG week–week stability, echocardiographic visualization of cuff constriction blood flow turbulence, and clinical observations of the pig. PG 'drift' above 80 mmHg resulted in two early deaths. Subsequently high PG ($>$80 mmHg) or rapidly drifting PG ($>$20 mmHg increments from preceding week) triggered partial cuff release. There was need for daily clinical observations particularly during the latter weeks of the protocol with vigilance for lethargy, tachypnea, cough, laboured breathing, and cyanosis. When present, we responded with supportive therapy (e.g. frusemide) and/or partial cuff release. All pigs that developed significant LVH over the 5–6 week study period were adjudicated to have pre-clinical, incipient HF with ~one-third decompensating to frank HF. This model produces more stable LVPO-induced HFpEF than our previously published model in sheep that used an acute onset aortic constriction (suprarenal) resulting in severe pre-morbid (euthanized) or terminal HF in all sheep with a variable but short (median 15 days) survival time.")[OAurl][?–]>")[OAurl][?–]>[9]

Although CMRI provides superior image resolution, echocardiography is non-invasive and economical. Echocardiography was used for frequent serial imaging of changes in cardiac structure and function. LV$_{mass}$/BW and LV wall thickness increased progressively in concert with transconstriction PGs. In contrast, LV volumes and LVEF showed no consistent change, indicating no significant LV dilation and preserved EF. Comparison of MRI and echocardiography generally showed equivalence of measurements. MRI allowed accurate measurement of left atrial volume, which increased in the cuff-LVH pigs, and assessment of cardiac fibrosis. Myocardial fibrosis impinges adversely on cardiac structure and function through increased myocardial stiffness and diastolic dysfunction,")[OAurl][?–]>")[OAurl][?–]>[10] impaired LV contraction and systolic dysfunction,")[OAurl][?–]>")[OAurl][?–]>[11] arrhythmias,")[OAurl][?–]>")[OAurl][?–]>[12] and impaired coronary blood flow")[OAurl][?–]>")[OAurl][?–]>[13] and is a powerful indicator of adverse outcomes in heart disease.")[OAurl][?–]>")[OAurl][?–]>[14,15] Spinale/Zile had previously demonstrated LVH in the LVPO model is associated with increased myocardial stiffness (three-fold) and total collagen (1.5-fold).")[OAurl][?–]>")[OAurl][?–]>[6] MRI T1 MOLLI results here clearly demonstrated global increases fibrosis across 16/17 segments of the LV. Only the apical lateral segment failed to show a definitive rise in T1 value. Nevertheless, picrosirius red staining at this site demonstrated significant collagen deposition (*Figure* ")[OAurl][?–]>")[OAurl][?–]>[6]), but rather than representative, it likely underestimated overall ventricular fibrosis in this model.

Invasive pressures measured in a subset of the LVH-cuff animals indicated elevations of PCWP and LVEDP to levels equivalent to those observed in mild–moderate clinical HF. The BNPs are long established biomarkers for the

diagnosis and prognosis of HF.")[OAurl][?–]>")[OAurl][?–]>[16] We used our well-validated assay for porcine/ovine BNP")[OAurl][?–]>")[OAurl][?–]>[8] to find elevated mean BNP levels with three samples from three pigs in the mild range (6–10 pmol/L or 21–35 pg/mL) and five in the moderate–severe HF range ($>$10 pmol/L or $>$~35 pg/mL, range of 39–119 pg/mL). Using the identical assay, sheep with post-myocardial infarction LV dysfunction have BNP levels of 10–12 pmol/L (~35–42 pg/mL),")[OAurl][?–]>")[OAurl][?–]>[17] and sheep with LVPO leading to pre-morbid (euthanasia) severe HF/death have BNP of 15.3 $\pm$ 3.6 pmol/L (~53 pg/mL).")[OAurl][?–]>")[OAurl][?–]>[9] Thus, levels of BNP measured in the pigs in this study were indicative of moderate to severe HF.

A highly novel aspect of this study is the HP[13]CMR imaging. Advanced cardiometabolic imaging allows detection of novel structural and metabolic cardiac changes. HP[13]CMR spectroscopy allows real-time study of myocardial energetics and substrate utilization to aid in understanding the pathophysiology of HFpEF and may identify novel therapeutic strategies. HP[13]CMR results showed significant increases in hyperpolarized [1-^{13}C]alanine and [^{13}C]bicarbonate levels in the cardiac tissue of HFpEF pigs. Because these [^{13}C]labeled metabolite signals of [1-^{13}C]lactate, [1-^{13}C]alanine, and [^{13}C] bicarbonate are obtained by conversion from the hyperpolarized injected [1-^{13}C]pyruvate via lactate dehydrogenase, ALT, and PDH, respectively, we deduced that ALT and PDH activity increased in the HFpEF pigs. The failing heart switches its energy source from fatty acids towards glucose,")[OAurl][?–]>")[OAurl][?–]>[18] directed towards glycolysis, whilst the change in glucose oxidation associated with PDH flux is related to the stage and pathogenesis of HF.")[OAurl][?–]>")[OAurl][?–]>[19] In rats with aortic constriction, glucose oxidation is initially increased, but eventually decreases as cardiac systolic dysfunction develops.")[OAurl][?–]>")[OAurl][?–]>[20] This may explain the increase in PDH flux in our HFpEF pig model. Others have demonstrated that in 8 weeks, from pressure-overload LVH non-diabetic rats, more active PDH complex was extracted compared with healthy hearts.")[OAurl][?–]>")[OAurl][?–]>[21] Increased cardiac glucose oxidation is also observed in spontaneously hypertensive rats")[OAurl][?–]>")[OAurl][?–]>[22] and in dogs with pacing-induced HF.")[OAurl][?–]>")[OAurl][?–]>[23] Concomitantly, increased ALT activity may reflect increased supply of amino acids and nucleic acids for hypertrophic growth.")[OAurl][?–]>")[OAurl][?–]>[20] Mice with LVH induced by aortic constriction show increased activation of anaplerotic pathways.")[OAurl][?–]>")[OAurl][?–]>[24] Taken together, the HP[13]CMR results indicate our porcine HFpEF model displays metabolic changes consistent with HF.

The unmet need for models of HFpEF allowing both elucidation of the biology of this syndrome and providing a test bed for candidate novel therapies has triggered interest in developing large animal models of HFpEF. Efforts in this direction have had varying degrees of success. In addition to the progressive LVPO model,")[OAurl][?–]>")[OAurl][?–]>[6] and our previously described sheep model of acute aortic constriction, which induced rapid deterioration to HF/death,")[OAurl][?–]>")[OAurl][?–]>[9] others have also employed aortic constriction in pigs. Acute onset aortic constriction beyond the carotid bifurcation resulted in rapid induction of LVH with reduced LVEF and acute HF by Day 7 (including death in 4/22 pigs), which then over 7 weeks evolved into a compensated phase of concentric LVH with restored cardiac function.")[OAurl][?–]>")[OAurl][?–]>[25] Thus, there is need to induce LVPO in a progressive nature as implemented in this study to induce progressive LVH without systolic dysfunction. Other authors banded ascending aorta of minipigs (25–30 kg) but showed no significant LVH or change in left atrial volume or LVEDP over 20 weeks and did not report of plasma BNP. Hence this effort produced no objective evidence of HF.")[OAurl][?–]>")[OAurl][?–]>[26] The Mayo group showed that renal wrapping of old dogs induced chronic hypertension with secondary LVH and fibrosis with impaired LV relaxation but no increase in LV diastolic stiffness claiming to mimic HFpEF.")[OAurl][?–]>")[OAurl][?–]>[27] However, the requirement for old animals (aged 8–13) makes this model relatively impractical and expensive.

The traditional rodent deoxy-corticosterone acetate (DOCA)–salt model has been upscaled to pigs, with variable results.")[OAurl][?–]>")[OAurl][?–]>[28,29] DOCA-salt pigs demonstrated significant increases in LV mass and wall thickness and also left atrial volumes at rest compared with control pigs.")[OAurl][?–]>")[OAurl][?–]>[28] During dobutamine stress, changes in LVEF and LVESV demonstrated normal contractile reserve but there were differences in cardiac index and LVEDV compared to normal pigs indicating inadequate increase in myocardial perfusion reserve during dobutamine stress perhaps indicating early-stage HFpEF but there was no change in T1 mapping of fibrosis.")[OAurl][?–]>")[OAurl][?–]>[28] When DOCA-induced hypertension is combined with high salt, fat, cholesterol, and sugar diet, pigs develop concentric LVH and left atrial dilation with no change in LVEF or HF symptoms at rest.")[OAurl][?–]>")[OAurl][?–]>[29] Whilst there was some evidence of pressure volume relationship being perturbed, LVEDP was not elevated unless pigs were challenged with pacing plus dobutamine. A recently reported study took an even more complex approach with multiple co-morbidities modelled by combining streptozocin-induced diabetes, renal artery embolization to induce kidney dysfunction and hypertension, and a high fat/salt diet in six pigs followed for 6 months.")[OAurl][?–]>")[OAurl][?–]>[30] They documented evidence of systemic inflammation, coronary endothelial dysfunction, and a rise in reactive oxygen species with disruption of nitric oxide along with myocardiocyte stiffness and cardiac fibrosis. This model claimed to be a clinically relevant model LV diastolic dysfunction and a precursor for HFpEF, but no pigs demonstrated overt HF. Thus, although

several large animal models have been proposed, none of these fulfil all the features present in human disease. That being said, human HFpEF is a complex syndrome with multiple contributing aetiologies with varying occurrence and severity of comorbidities. Animal models invariably model some but not all aspects of pathology, thus, researchers need to select combinations of pathological features according to the specific aims of their study. Many of the models noted above replicate pre-clinical disease with no objective evidence of HF; thus, they represent early stages of the disease process and not HFpEF *per se*.

In conclusion, we have described a steadily progressive, but sufficiently stable and controllable (via titration of cuff/constriction) model of LVPO with novel data evidencing fibrosis based on MRI T1 MOLLI mapping, elevated filling pressures, metabolic changes, and progression to frank HF with prolongation of the model. This is a clinically relevant model of HFpEF on a predominant background of hypertension with clear utility in advancing knowledge of underlying pathophysiology of HFpEF and testing novel candidate therapies.

References

1. McMurray JJV, Adamopoulos S, Anker SD, Auricchio A, Bohm M, Dickstein K, Falk V, Filippatos G, Foneseca C, Gomez-Sanchez MA, Jaarsma T, Kober L, Lip GY, Maggioni AP, Parkhomenko A, Pieske BM, Popescu BA, Ronnevik PK, Rutten FH, Schwitter J, Sererovic P, Stepinska J, Trindade PT, Voors AA, Zannad F, Zeiher A, ESC Committee for Practice Guidelines. ESC Guidelines for the diagnosis and treatment of acute and chronic heart failure 2012: The task force for the diagnosis and treatment of acute and chronic heart failure 2012 of the European Society of Cardiology. Developed in collaboration with the Heart Failure Association (HFA) of the ESC. *Eur Heart J* 2012; **33**: 1787–1847.

2. Lam CSP, Gamble GD, Ling LH, Sim D, Leong KTG, Yeo PSD, Ong HY, Jaufeerally F, Ng TP, Cameron VA, Poppe K, Lund M, Devlin G, Troughton R, Richards AM, Doughty RN. Mortality associated with heart failure with preserved vs. reduced ejection fraction in a prospective international multi–ethnic cohort study. *Eur Heart J* 2018; **39**: 1770–1780.

3. Zheng SL, Chan FT, Nabeebaccus AA, Shah AM, McDonagh T, Okonko DO, Ayis S. Drug treatment effects on outcomes in heart failure with preserved ejection fraction: a systematic review and meta–analysis. *Heart* 2018; **104**: 407–415.

4. Roh J, Houstis N, Rosenzweig A. Why don't we have proven treatments for HFpEF. *Circ Res* 2017; **120**: 1243–1245.

5. Conceicao G, Heinonen I, Lourenco AP, Duncker DJ, Falcao-Pires I. Animal models of heart failure with preserved ejection fraction. *Neth Heart J* 2016; **24**: 275–286.

6. Yarbrough WM, Mukherjee R, Stroud RE, Rivers WT, Oelsen JM, Dixon JA, Eckhouse SR, Ikonomidis JS, Zile MR, Spinale FG. Progressive induction of left ventricular pressure overload in a large animal model elicits myocardial remodeling and a unique matrix signature. *J Thorac Cardiovasc Surg* 2012; **143**: 215–223.

7. Stefan D, Di Cesare F, Andrasescu A, Popa E, Lazariev A, Vescovo E, Strbak O, Williams S, Starcuk Z, Cabanas M, van Ormondt D, Graveron-Demilly D. Quantitation of magnetic resonance spectroscopy signals: the jMRUI software package. *Measurement Sci Tech* 2009; **20**: 104035 (9 pp).

8. Pemberton CJ, Yandle TG, Charles CJ, Rademaker MT, Aitken GD, Espiner EA. Ovine brain natriuretic peptide in cardiac tissues and plasma: effects of cardiac hypertrophy and heart failure on tissue concentration and molecular forms. *J Endocrinol* 1997; **155**: 541–550.

9. Charles CJ, Kaaja RJ, Espiner EA, Nicholls MG, Pemberton CJ, Richards AM, Yandle TG. Natriuretic peptides in sheep with pressure overload left ventricular hypertrophy. *Clin Exp Hypertens* 1996; **18**: 1051–1071.

10. Zile MR, Baicu CF, Ikonomidis JS, Stroud RE, Nietert PJ, Bradshaw AD, Slater R, Palmer BM, Van Buren P, Meyer M, Redfield MM, Bull DA, Granzier HL, LeWinter MM. Myocardial stiffness in patients with heart failure and a preserved ejection fraction: contributions of collagen and titin. *Circulation* 2015; **131**: 1247–1259.

11. Querejeta R, López B, González A, Sanchez E, Larman M, Martinez Ubago L, Diez J. Increased collagen type I synthesis in patients with heart failure of hypertensive origin: relation to myocardial fibrosis. *Circulation* 2004; **110**: 1263–1268.

12. Takarada A, Yokota Y, Fukuzaki H. Analysis of ventricular arrhythmias in patients with dilated cardiomyopathy—relationship between the effects of antiarrhythmic agents and severity of myocardial lesions. *Jpn Circ J* 1990; **54**: 260–271.

13. Dai Z, Aoki T, Fukumoto Y, Shimokawa H. Coronary perivascular fibrosis is associated with impairment of coronary blood flow in patients with non–ischemic heart failure. *J Cardiol* 2012; **60**: 416–421.

14. Azevedo CF, Nigri M, Higuchi ML, Pomerantzeff PM, Spina GS, Sampaio

RO, Tarasoutchi F, Grinberg M, Rochitte CE. Prognostic significance of myocardial fibrosis quantification by histopathology and magnetic resonance imaging in patients with severe aortic valve disease. *JACC* 2010; **56**: 278–287.

15. Aoki T, Fukumoto Y, Sugimura K, Oikawa M, Satoh K, Nakano M, Nakayama M, Shimokawa H. Prognostic impact of myocardial interstitial fibrosis in non–ischemic heart failure. Comparison between preserved and reduced ejection fraction heart failure. *Circ J* 2011; **75**: 2605–2613.

16. Richards AM. Future biomarkers in cardiology: My favourites. *Eur Heart J Suppl* 2018; **20**: G37–G44.

17. Rademaker MT, Cameron VA, Charles CJ, Espiner EA, Nicholls MG, Pemberton CJ, Richards AM. Neurohormoes in an ovine model of compensated postinfarction left ventricular dysfunction. *Am J Physiol* 2000; **278**: H731–H740.

18. Sankaralingam S, Lopaschuk GD. Cardiac energy metabolic alterations in pressure overload–induced left and right heart failure (2013 Grover Conference Series). *Pulm Circ* 2015; **5**: 15–28.

19. Doenst T, Nguyen TD, Abel ED. Cardiac metabolism in heart failure: implications beyond ATP production. *Circ Res* 2013; **113**: 709–724.

20. Doenst T, Pytel G, Schrepper A, Amorim P, Färber G, Shingu Y, Mohr FW, Schwarzer M. Decreased rates of substrate oxidation ex vivo predict the onset of heart failure and contractile dysfunction in rats with pressure overload. *Cardiovasc Res* 2010; **86**: 461–470.

21. Lydell CP, Chan CP, Wambolt RB, Sambandam N, Parsons H, Bondy GP, Rodrigues B, Popov KM, Harris RA, Brownsey RW, Allard MF. Pyruvate dehydrogenase and the regulation of glucose oxidation in hypertrophied rat hearts. *Cardiovasc Res* 2002; **53**: 841–851.

22. Dodd MS, Ball DR, Schroeder MA, Le Page LM, Atherton H, Heather LC, Seymour AM, Ashrafian H, Watkins H, Clarke K, Tyler DJ. In vivo alterations in cardiac metabolism and function in the spontaneously hypertensive rat heart. *Cardiovasc Res* 2012; **95**: 69–76.

23. Osorio JC, Stanley WC, Linke A, Castellari M, Diep QN, Panchal AR, Hintze TH, Lopaschuk GD, Recchia FA. Impaired myocardial fatty acid oxidation and reduced protein expression of retinoid X receptor–alpha in pacing–induced heart failure. *Circulation* 2002; **106**: 606–612.

24. Kolwicz SC Jr, Olsen DP, Marney LC, Garcia-Menendez L, Synovec RE, Tian R. Cardiac–specific deletion of acetyl CoA carboxylase 2 prevents metabolic remodeling during pressure–overload hypertrophy. *Circ Res* 2012; **111**: 728–738.

25. Xiong Q, Zhang P, Guo J, Swingen C, Jang A, Zhang J. Myocardial ATP hydrolysis rates in vivo: a porcine model of pressure overload–induced hypertrophy. *Am J Physiol* 2015; **309**: H450–H458.

26. Hiemstra JA, Liu S, Ahlman MA, Schuleri KH, Lardo AC, Baines CP, Dellsperger KC, Bluemke DA, Emter CA. A new twist on an old idea: a two–dimensional speckle tracking assessment of cyclosporine as a therapeutic alternative for heart failure with preserved ejection fraction. *Physiol Rep* 2013; **1**: e10074.

27. Hamdani N, Bishu KG, von Frieling-Salewsky M, Redfield MM, Linke WA. Deranged myofilament phosphorylation and function in experimental heart failure with preserved ejection fraction. *Cardiovasc Res* 2013; **97**: 464–471.

28. Reiter U, Reiter G, Manninger M, Adelsmayr G, Schipke J, Alogna A, Rajces A, Stalder AF, Greiser A, Muhlfeld C, Scherr D, Post H, Pieske B, Fuchsjager M. Early–stage heart failure with preserved ejection fraction in the pig: a cardiovascular magnetic resonance study. *J Cardiovasc Magn Reson* 2016; **18**: 63–78.

29. Schwarzl M, Hamdani N, Seiler S, Alogna A, Manninger M, Reilly S, Zirngast B, Kirsch A, Steendijk P, Verderber J, Zweiker D, Eller P, Hoffler G, Schauer S, Eller K, Maechler H, Pieske BM, Linke WA, Casadei B, Post H. A porcine model of hypertensive cardiomyopathy: implications for heart failure with preserved ejection fraction. *Am J Physiol* 2015; **309**: H1407–H1418.

30. Sorop O, Heinonen I, van Kranenburg M, van de Wouw J, de Beer VJ, Nguyen ITN, van Duin RWB, Stam K, van Geuns R-J, Wielopolski PA, Krestin GP, van den Meiracker AH, Verjans R, van Bilsen M, Danser AHJ, Paulus WJ, Cheng C, Linke WA, Joles JA, Verhaar MC, van der Velden J, Merkus D, Duncker DJ. Multiple common comorbidities produce left ventricular diastolic dysfunction associated with coronary microvascular dysfunction, oxidative stress, and myocardial stiffening. *Cardiovasc Res* 2018; **114**: 954–964.